

A Forward Model of Mantle Convection with Evolving Continents and a Model of the Andean Subduction Orogen

Uwe Walzer, Roland Hendel, Christoph Köstler, Markus Müller, Jonas Kley, and Lothar Viereck-Götte

Abstract Some essential features of Andean orogenesis cannot be explained *only* by a dynamic *regional* model since there are essential influences across its vertical boundaries. A dynamic regional model of the Andes should be embedded in a 3-D spherical-shell model. Because of the energy distribution on the poloidal and toroidal parts of the creep velocity and because of geologically determined mass transport alongside the Andes, both models have to be three-dimensional. Furthermore, we developed a new viscosity profile of the mantle with very steep gradients at the lithospheric-asthenospheric boundary and at a depth of 410 and 660 km. Therefore, the challenges to the code Terra are now essentially larger. In the last 3 years we have resolved these problems in an international cooperation (see Sect. 2.2). Based on the new viscosity profile and on an improved Terra, we computed a new forward spherical-shell model (Walzer and Hendel, J Geophys Res submitted, 2012b). For this model, we derived also a new extended acoustic Grüneisen parameter, γ_{ax} , new profiles of the thermal expansivity, α , and of the specific heat, c_v , at constant volume as well as a solidus depending on both the pressure and the water abundance. These innovations are essential to incorporate a chemical-differentiation mechanism into the model. We arrived at rather realistic episodes of continental growth interrupted by magmatically quiet time spans distributed over the whole time axis. Nevertheless, the model shows a main magmatic event at the very beginning of the Earth's evolution. Papers on the improvement of Terra (Köstler et al. Comput Geosci submitted, 2012; Müller and Köstler, Int J Numer Methods Eng submitted, 2012) have been written. We conceived a regional model of the Andean orogenesis (Sect. 3.2.1) with the same new viscosity profile. We want to investigate why there is flat-slab subduction in some segments of the Andes and why deformation of the crust and volcanism migrate eastward. The evolution of

U. Walzer (✉) · R. Hendel · C. Köstler · M. Müller · J. Kley · L. Viereck-Götte
Institut für Geowissenschaften, Friedrich-Schiller-Universität, Humboldtstr. 11,
07743 Jena, Germany
e-mail: u.walzer@uni-jena.de

the abundances of incompatible elements indicate a cycle which was finished by a fast process, perhaps by a large-scale delamination of the lower plate, perhaps also by another type of delamination. In connection with another spherical-shell model (with prescribed plate boundaries), the regional model should numerically explain why a plateau-type orogen evolved at an oceanic-continental plate boundary.

1 Introduction

The papers which refer to our topic can be classified by seven subjects.

- (a) Geological description of dynamic problems of thermal evolution of the Earth, plate tectonics and chemical differentiation as well as of the Andean orogeny,
- (b) Models which are partially kinematic and partially dynamic. In this kind of models, essential features are prescribed in order to gain a large adaptation to geological and geophysical observations.
- (c) Geochemical models of growth and differentiation of continents which do not contain any dynamic modeling,
- (d) Dynamic models of the subduction process to understand the physical mechanism behind subduction,
- (e) Circulation models,
- (f) Fully dynamic models of subduction in a diamond (cf. Fig. 8), i.e. in a certain 3-D sector of the spherical shell, which represents the mantle, where this diamond is embedded into a realistic 3-D spherical-shell solution,
- (g) Fully dynamic forward models of spherical-shell convection with chemical differentiation and generation of continents.

We systematically described the papers of types (a)–(e) in [110]. Therefore, we will not repeat it here. Up to now, there is no paper of type (f). Some supplements will follow: To obtain a more profound analysis of the Andean orogeny, it is important to understand why a plateau-type orogen formed between a purely oceanic lithospheric plate (Nazca plate) and a continent (South America) [71]. The Andean mountain belt belongs to the non-collisional type. Kley and Monaldi [42,45,46] found a Cenozoic shortening of 250–350 km whereas Arriagada et al. [4] derived 400 km for the central Andes. In other areas of the Earth, however, the subduction zones at an oceanic-continental plate-boundary site have only little or no shortening and do not show any elevated plateaus. In most cases, the upper plate is characterized by backarc extension. Schellart and Rawlinson [82] discuss some hypotheses of which it is claimed that they explain this exceptional behavior of the Andes.

- In [66], it is proposed that the young age of the Nazca plate and low negative buoyancy cause this phenomenon.

- Climatic conditions, high friction and subduction erosion is thought to be the decisive factor [57, 58].
- Heuret and Lallemand [30] emphasize the eminent role of acceleration of the westward movement of the upper, South American plate. Sobolev et al. [84] find out that the accelerating westward movement of the South American plate is the most important factor for the Andean orogeny.

The third hypothesis generates the question of the mechanism which drives South America westward. The ridge push at the mid-Atlantic ridge and the slab pull at the Lesser Antilles and the Scotia arc have been proposed but it could be that these contributions are too small. Schellart and Rawlinson [82] remarkably mention the slab pull of the Nazca plate. However, we propose that a downwelling of the bulk convection beneath South America caused by the thermal screening of the thick continental lithosphere could play a role. If there is a large upwelling east of South America and a large downwelling of the bulk convection under South America we could understand why the bulk convection current would move the South American plate westward since, because of the thick continental lithosphere, South America is *not* decoupled from the bulk convection by the asthenosphere. Additionally, we observe a large upwelling of the bulk convection beneath the Pacific. So we can expect that another current of the bulk convection will go eastward, producing the arcs of the Lesser Antilles and Scotia. It is unclear if these speculative arguments are appropriate. However, they show not only the necessity of dynamic, numerical regional models but also that the regional model must be nestled among time dependent boundary conditions determined by a global dynamic model. Evidently, some *essential* features of the Andean orogenesis cannot be explained by an isolated regional model.

We discuss further *new* geological and geophysical papers in Sect. 3.2.1. We did that on purpose in order to substantiate why we used certain details in our development of two special (alternative) mechanisms for a regional model of the South American subduction zone and Andean orogenesis. Further *new* papers are mentioned in Sect. 3.2.2 in order to select an appropriate set of prescribed plate movements in the surrounding spherical-shell convection model which is necessary to embed the regional model.

2 A Spherical-Shell Forward Model and Other Results

Under Sects. 2.1–2.3, we describe what we have done using the system HP XC4000 of the Steinbuch Center for Computing in Karlsruhe. Under Sect. 2.4, other efforts of us which have some relation to the topic are reported. There is a direct relationship between the Sect. 2.1–2.3 and the running works which we describe in Sect. 3.2.1 in rather distinct outlines, i.e. we discuss our specific South American dynamical model which is embedded in a second spherical-shell model.

2.1 Spherical-Shell Model: Forward Model

We developed two spherical-shell convection models. The forward model is described here; another model with prescribed plate movements is outlined under Sect. 3.2.2. For both spherical-shell models as well as for the regional models of the Andes (Sect. 3.2.1), we newly derived, in some cases adopted new radial profiles of the relevant physical parameters of the mantle [101]. As a Grüneisen parameter, we calculated an extended acoustic gamma, γ_{ax} , using seismic observations. These observed values are the bulk modulus K , the shear modulus μ , dK/dP and $d\mu/dP$, where P is the pressure. This procedure has the advantage to be based on observable quantities without any assumptions on mineralogy. A further calculated property is the adiabatic gradient. We derived new profiles for the thermal expansivity, α , and the specific heat, c_v , at constant volume. For the chemical differentiation we used a simple melting criterion, $T > f_3 \cdot T_m$, where T is the temperature and T_m is the solidus. We estimated the lower-mantle solidus using values of [60] and of other authors continuing them by using our γ_{ax} . In the upper mantle and the transition layer, we took into consideration the water dependence of the solidus. Litsov [61] investigated the influence of different water concentrations on the solidus of peridotite and we took the derived depressions of the solidi into account in the computation of our convection-differentiation model of the mantle's evolution. So in our new model, the melting temperature is a function of time and position. The most important innovation of the new convection model concerns our newly derived viscosity profile which is based on solid-state physics and seismological results [100, 101]. This viscosity distribution has a resemblance to the viscosity model of [65] although its derivation is totally different. The full set of convection-differentiation equations has been solved using the improved code Terra (see Sect. 2.2). For each run, we obtained lots of parameters, some of which can be compared with observational quantities. For ages from 4,490 Ma to the present time, we received the curves of the laterally averaged heat flow density q_{ob} at the surface, the converted continent-tracer mass per Ma, the Urey number Ur , the Rayleigh number Ra , the Nusselt number Nu , the volumetrically averaged mean temperature T_{mean} of the mantle, showing a very realistic temperature drop when compared with Archean komatiite temperatures, the integrated mass of continents, the kinetic energy of the mantle flow E_{kin} , the radiogenic heat production Q_{bar} and the laterally averaged heat flow density q_{cmb} at the core-mantle boundary (CMB). Further results are the vector field of the creeping velocity and the temperature distribution for every time step of the Earth's evolution. Up to now, we varied the melting parameter f_3 and the thermal conductivity k . There are $f_3 - k$ clusters of realistic totalities of solutions. Figure 1 represents an episodic distribution of juvenile additions to the continents which is connected with the episodicity of orogenic epochs. Figure 2 shows the present-day distribution of continents of the same run. In this example, 42.2 % of the Earth's surface is covered by continents. The present-day surface heat flow of this run is 81.39 mW/m², comparable with the observed value of 90.185 mW/m² [12]. The present-day value of q_{cmb} of this run is 20.20 mW/m² which seems to be realistic, too.

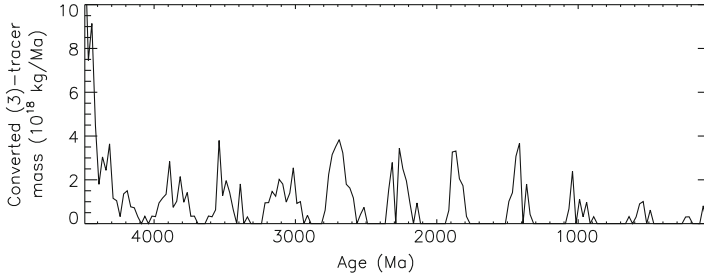


Fig. 1 Juvenile additions to the sum of continental masses acc. to the *new* convection-differentiation model Run 498, [101]

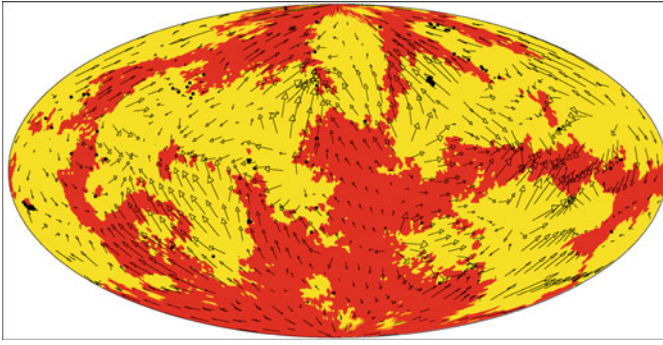


Fig. 2 The distribution of continents (red), oceanic lithosphere (yellow) and oceanic plateaus (black dots) for the present time according to the *new* convection-differentiation model [101], Run 498, $r_n = 0.5$, $\sigma_y = 120$ MPa, continental percentage = 42.2%

We computed the shear viscosity, η , using

$$\eta(r, \theta, \phi, t) = 10^{r_n} \cdot \frac{\exp(c \frac{T_m}{T_{av}})}{\exp(c \frac{T_m}{T_{st}})} \cdot \eta_4(r) \cdot \exp \left[c_l \cdot T_m \left(\frac{1}{T} - \frac{1}{T_{av}} \right) \right] \quad (1)$$

where r is the distance from the Earth's mass center, θ the colatitude, ϕ the longitude, t the time and r_n the viscosity-level parameter. The quantity r_n has been varied to shift the viscosity profile to the left or to the right. So we generated different time-averaged Rayleigh numbers, Ra , varying from run to run. T_m is the newly invented melting temperature [101] which additionally depends on water abundance. So T_m is a function of time, too. T_{av} is the laterally averaged temperature, T_{st} the initial temperature profile. The quantity η_4 denotes the new viscosity profile [101] for the initial temperature and $r_n = 0$. For MgSiO_3 perovskite we should insert $c = 14$, for MgO wüstite $c = 10$ according to [113]. Therefore, the lower-mantle value of c should be somewhere between these two values. For numerical reasons, however, we are able to use only $c = 7$. In the lateral-variability term we use $c_l = 1$. The temperature is denoted by T .

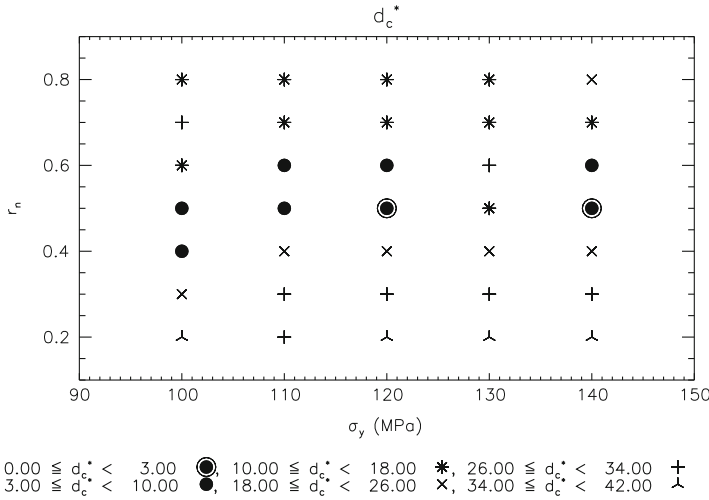


Fig. 3 We compare different runs which are distinguished only by the viscoplastic yield stress, σ_y , and the viscosity-level parameter r_n . The *symbols* represent the magnitude of the difference, d_c^* , between the computed and observed present-day surface percentage of continents, expressed in percent

Figure 3 shows the difference between computed and observed present-day continental surface percentage. The central run with $r_n = 0.5$ (corresponding to $Ra \approx 10^8$) and $\sigma_y = 120$ MPa has the minimum difference between theory and observation, namely 1.85%. This run shows also other optimal results, e.g. regarding the temporal distribution of the magmatic-activity episodes (cf. Fig. 1) and the (spectral) distribution of continents (cf. Fig. 2). Further variations of the parameters refer to the factor f_3 of the melting criterion and to the thermal conductivity, k , keeping r_n and σ_y fixed at the mentioned two values. At a first glance on Fig. 4, we could have the impression that there is a trade-off between k and f_3 since optimal solutions (black circles with an outer ring) cluster along a certain curve. But all the other observable quantities in other $f_3 - k$ plots show that only the three optimum solutions with $k = 5.0$ W/(m·K) in the upper right corner of Fig. 4 are realistic. Figure 5 demonstrates, e.g., that only thermal-conductivity values around $k = 5.0$ W/(m·K) lead to solutions which are satisfactory for *all* observables. This value is acceptable also from the physical point of view [115]. Therefore, we varied f_3 in small steps from 1.000 downward, keeping $k = 5.0$ W/(m·K). As expected from Figs. 4 and 5 and similar $f_3 - k$ plots we obtained very realistic solutions down to $f_3 = 0.985$. However, already $f_3 = 0.983$ and $f_3 = 0.981$ generates less convincing results. Figure 6, e.g., shows the corresponding present-day distribution of continents.

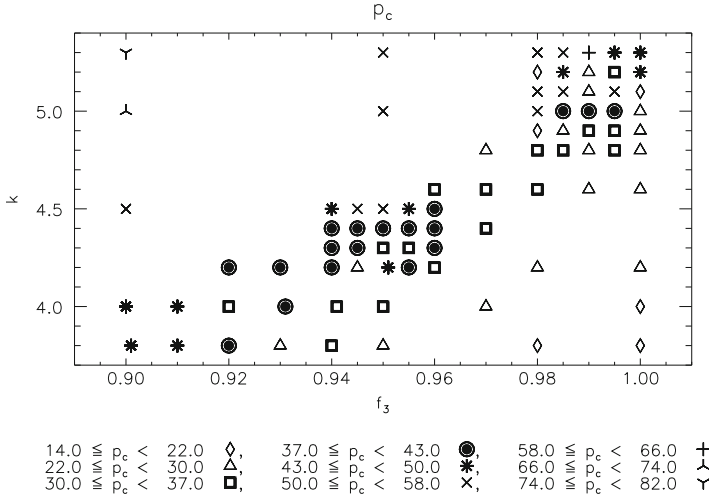


Fig. 4 Keeping $r_n = 0.5$ and $\sigma_y = 120$ MPa fixed, we vary the melting-criterion factor, f_3 , and the thermal conductivity, k . The symbols represent intervals of the theoretical present-day continental surface, p_c , in percent. Note for comparison that 40.35% of the real present-day Earth is covered by continents and epicontinental seas. The optimal run, shown in Figs. 1 and 2, corresponds to $k = 5.0$ W/(m·K) and $f_3 = 0.995$

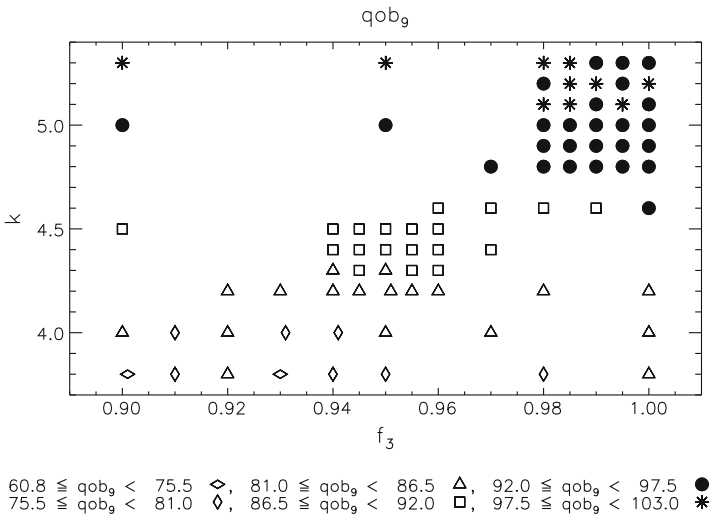


Fig. 5 A $f_3 - k$ plot for constant $r_n = 0.5$ and $\sigma_y = 120$ MPa. The laterally averaged surface heat flow is denoted by qob . The temporal average of qob over the last 900 Ma is called qob_9 and is expressed in mW/m^2

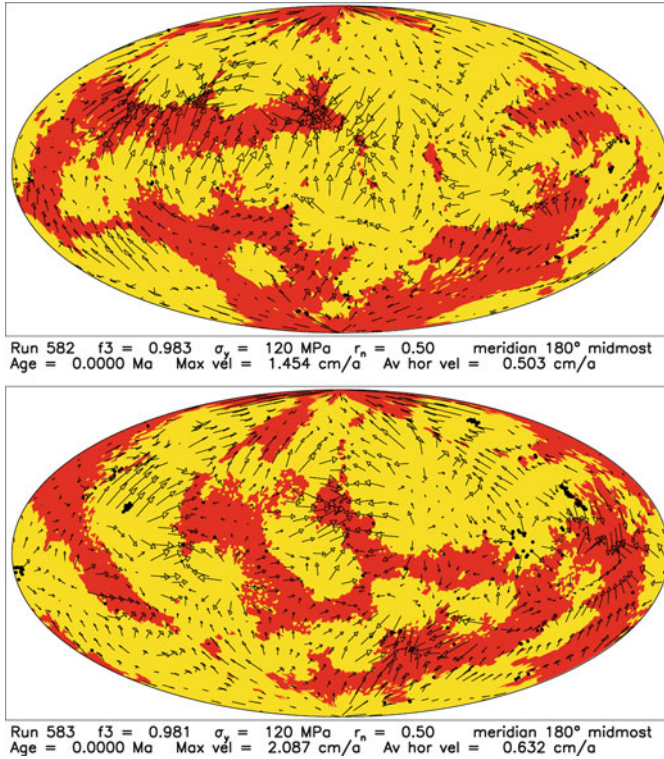


Fig. 6 Less realistic distributions of continents (*red*), oceanic lithosphere (*yellow*) and oceanic plateaus (*black dots*) for the present time. $r_n = 0.5$, $\sigma_y = 120$ MPa, $k = 5.0$ W/(m·K), $f_3 = 0.983$ and $f_3 = 0.981$, respectively

2.2 Numerical Improvements

Two submitted publications of our group [55,69] deal with *numerical improvements*. Their conclusions will not be discussed here. However, their results are very important for the realization of our Andean model (Sect. 3.2.1).

A big part of our efforts was concentrated on the creation of an essentially improved Terra code, which is necessary to resolve the numerical problems with the newly derived viscosity profiles. We equally apply this new viscosity profile [101] to a spherical-shell mantle convection model [100, 101] as well as to the regional model of the South American subduction slabs (Sect. 3.2.1). In 2009, the Terra developers of the universities Munich (H.-P. Bunge, M. Mohr), Cardiff (H. Davies), Leeds (P. Bollada), Jena (M. Müller, C. Köstler) and of the Imperial College London (R. Davies) and others started a close cooperation in the further development of the Terra code and intensified the collaboration with J. Baumgardner (San Diego, USA), the inventor of Terra. At a first joint meeting in Munich in 2009, the group decided

to set up a community svn-repository for further code development, supplemented by trac, a web-based project management and bug-tracking tool, and automated compile/test cycles using BuildBot. From then on the group worked on a common code base using automated tests for every revision of the code. There have been three successive joint meetings in Cardiff in 2010, in Jena in 2011 (see also <http://www.igw.uni-jena.de/geodyn/terra2011.html>) and in Munich in 2012. The progress being made since the first meeting includes the following items.

- Enhancement of the code to increase global resolution and maximum number of MPI processes.
- Further development and integration of the Ruby test framework [68] into the automated BuildBot tests.
- Implementation of a finite-element inf-sup stabilization using pressure-polynomial projections proposed in [15].
- Development and implementation of an efficient preconditioner for the variable-viscosity Stokes system [54].
- Refinement of the Pressure Correction algorithm [54], giving more robust convergence.
- Restructuring of the code to use language features of Fortran95 and Fortran2003 where possible.
- Integration of automated code documentation using doxygen.
- Integration of VTK-support and automated visualization.
- Significant improvements in the formulation of the free-slip boundary condition on the spherical surface.

Continued effort is spent on several numerical and technical topics as well as on including more realistic physical models. In the following, some important details are given.

- In [97, 100, 101], two pressure- and temperature-dependent viscosity profiles of the Earth's mantle are developed and used for the computation of two mantle convection models with chemical differentiation of oceanic plateaus and generation of continents. The new viscosity model includes very strong viscosity gradients at lithosphere-asthenosphere boundary and at 410- and 660-km phase boundaries. Therefore, it is very important to make the code Terra fit for such a strong challenge. Regarding a physically consistent variable viscosity momentum operator, J. Baumgardner, P. Bollada and C. Köstler figured out in which way the code has to be changed to apply a physically consistent A-operator using cell-averaged viscosities. The most significant code change is the switch from nodal based to triangle based operator parts on the sphere. The viscosity-weighted summation over triangular integrals is then done in the application of the operator. We expect that the cost for applying Au will be doubled but a consistent formulation on all grid-levels could pay off for this, especially if we get a better convergence rate of the multigrid algorithm. The implementation of the triangle-based operator formulation is now under way.

- Exporting Terra-operators in sparse matrix format: When exporting the FE-matrices for the whole grid, they can be analyzed and PETSc or other parallel solver packages can be applied to it. This is intended to provide flexibility and to ensure reliability of future code changes.
- Multigrid(MG)-implementation: As mentioned in [90], the current MG-implementation in Terra does not fulfill the expectations raised by the performance of a 2-D Cartesian version of Terra, documented in [114]. In [54] it is also identified to be the worst performing part of the iterative solver in Terra. It is only poorly analyzed, and it is not satisfactory documented. M. Mohr is going to analyze and document the currently used matrix-dependent transfer multigrid in detail. The MG-implementation is also to be changed to using cell-based viscosity averages.
- Free-slip boundary condition and propagator matrix benchmark tests: P. Bollada and R. Davies showed that adding boundary terms to the right hand side of the momentum equation reduces some sort of errors while other kinds of errors still exist. They will continue to figure out the exact cause of that behavior and work on fixing this. With direct access to the radial velocity component, the local spherical coordinate system offers a way to straightforward implement the free-slip boundary condition. J. Baumgardner implemented this in a local copy of Terra, and it is ready to be used. The group has agreed to create a repository branch to continue working on that. If successful, the local spherical coordinate system-version will be merged into the trunk after some months of testing.
- Adding Ruby tests: The Ruby test framework is ready to be used extensively in testing Terra's subroutines as individually as possible. It can also be used for debugging by application of subroutines to predefined scalar and vector fields. Still the test coverage of the Terra by Ruby tests is very low and needs to be extended.

2.3 Andean Model

A large expenditure of time of U. Walzer in the last 3 years was the analysis and synopsis of geophysics, geology and geochemistry of the Andean orogenies. This has been done in close cooperation with J. Kley and L. Viereck-Götte. Some geophysical and geological considerations are outlined in Sect. 3.2.1.

2.4 Long-Term Related Works of Our Group

Kley investigated the structural geology of some areas of the central Andes [40] and gave a regional structural analysis and kinematic restoration [41,47]. He participated in an effort to extend quantitative structural analysis to a transect right across the backarc area. First steps were also taken towards constraining the evolution of

strain rates over time [49], leading to the suggestion that the continental strain rates had increased during the Andean orogeny. Kley began to extend kinematic analysis to the entire orogen, employing serial balanced sections and map view restoration techniques [44]. A map view kinematic model of the central Andes [45] formed the basis for comparison of geologically derived, orogen-scale kinematics with GPS and seismologic data [31, 32, 52]. It could be shown that the present-day strain field from satellite geodetic data closely matches the strain field for the last 10 Ma as inferred from geologic evidence. Additional evidence was presented that the strain rate in the South American plate becomes independent of plate convergence rate in the later stages. Using the map-view strain field as input for a numerical model, an attempt was also made to constrain crustal thickness evolution and the flux of crustal material during the Andean orogeny [33]. The studies on variations in structural style along the Andes [42] also triggered a second line of research dealing with the influence of inherited lithospheric heterogeneities on the spatial strain distribution. One important factor here is the widespread occurrence of Mesozoic rift basins [50] that were partially inverted as the thrust front migrated across them. Several case studies from a particularly well-exposed rift system in northern Argentina helped to clarify the importance of fault reactivation and stratigraphic discontinuities in conditioning the mechanical behavior of the upper crust in contraction [43, 46, 51, 67]. The results of these studies were incorporated in [48, 71].

Walzer and cooperators worked on convection-fractionation problems. The thermal evolution of the mantle and the chemical evolution of the principal geochemical reservoirs have been modeled simultaneously by a fractionation mechanism plus 2D-FD thermal convection [93–96]. Oceanic plateaus, enriched in incompatible elements, develop leaving behind the depleted parts of the mantle. The resulting inhomogeneous heat-source distribution generates a first feed-back mechanism. The lateral movability of the growing continents causes a second feed-back mechanism [95]. Effects of the viscosity stratification on convection and thermal evolution of a 3D spherical-shell model have been investigated and a viscosity profile of the mantle was developed [103, 104]. The paper [106] presents 2D and 3D thermochemical models of mantle evolution where a self-consistent theory is included using the Helmholtz free energy, the Ullmann-Pan'kov equation of state, the free-volume Grüneisen parameter and Gilvarry's formulation of Lindemann's law. In order to obtain the relative variations of the radial factor of the shear viscosity, the pressure, P , the bulk modulus, K , and $\partial K / \partial P$ from the seismic model PREM have been used. The publications [97, 104, 105, 107] present models of self-consistent generation of stable, but time-dependent plate tectonics on a 3D spherical shell. Different types of solutions have been found for different models by systematic variation of parameters [97, 102, 104, 108, 109]. Stirring effects are investigated in [22]. A 3D spherical-shell mantle convection and evolution model with growing continents [97, 100, 101, 108, 109] has been developed. The evolution model equations guarantee conservation of mass, momentum, energy, angular momentum, and of four sums of the numbers of atoms of the pairs ^{238}U - ^{206}Pb , ^{235}U - ^{207}Pb , ^{232}Th - ^{208}Pb , and ^{40}K - ^{40}Ar . The pressure- and temperature-dependent viscosity is supplemented by a viscoplastic yield stress.

The lithospheric viscosity is partly imposed to mimic the viscosity increase by chemical layering and devolatilization. Stochastic effects [98] are shown to exist especially in the chemical differentiation. Although the convective flow patterns and the chemical differentiation of the oceanic plateaus are coupled, the evolution of the time-dependent Rayleigh number, Ra_t , is relatively well predictable from run to run and the stochastic parts of the $Ra_t(t)$ – curves are small [97].

Viereck-Götte and cooperators worked not only about the genesis of the Jurassic Ferrar large igneous province in Antarctica but also about the connection between Antarctica, South America and Africa. Plateau forming lavas in the Karoo province of South Africa and in the Ferrar province in Antarctica were emplaced synchronously at about 180 Ma. They thus seem to originate from the same dynamic mantle process. However, both are distinguished by their isotopic characteristics with respect to the Rb/Sr- and Sm/Nd systems: while the Karoo magmas show mantle values, the Ferrar magmas exhibit enriched upper crustal values. However, the boundary between both Jurassic igneous provinces is marked by a large transpressional shear zone (Heimefront SZ) of Pan-African age (600–500 Ma), crossing Dronning Maud Land (S-African side of Antarctica) on the continent side of the Grunehogna craton, a fragment of the W-Gondwana Transvaal craton. This shear zone is interpreted as a reactivated suture of Grenvillean age (1.1 Ga). If Jurassic magmas on either side of this boundary are isotopically different, it must be concluded that

1. This is not a signature in a lower mantle plume.
2. This must be a signature within the subcontinental lithospheric mantle.
3. This signature must be older than Grenvillean in age.
4. It must be introduced into a paleo supra-subduction mantle wedge by subduction processes if it is a crustal isotopic signature.

Their studies concentrated on the timing of the initiation of the Ferrar as a large igneous province as well as on the physicochemical characterization of the melt source region conditions during melt differentiation. Studying the intrusive, extrusive and volcanoclastic rocks:

- They reconstructed the initiation of a large igneous province to have occurred in several steps of melt pulses within 5 Ma (189–183 Ma ago).
- They showed initiation to have started with large-volume shallow-level intrusions of low-Ti andesitic melts into wet fluvial sediments (Triassic/Jurassic) associated with diatreme-forming Taalian-type eruptions.
- The eruptions followed by basaltic andesites in small volume eruptions of partly pillowed lavas from local eruptive centers prior to large volume plateau forming lava extrusions from feeder dikes followed by a final pulse of a large volume andesites high in Ti that had differentiated from a common primary melt under lower pressure, oxygen fugacity and water activity.

All melts belong to the tholeiitic differentiation series, however with orthopyroxene instead of olivine as early fractionating mafic solidus phase. REE, Sr-Nd-isotope and PGE characteristics indicate generation of the primary melts within the

spinel-lherzolite zone of an isotopically enriched and sulfur-undersaturated subcontinental lithospheric mantle. Crustal silica enrichment of this source due to an overprint in a supra-subduction environment had already been concluded from Re-Os isotopy. Our Sr-isotope data in plagioclase phenocrysts, however, exhibit decreasing radiogenic character in subsequent melt pulses indicating additional assimilation of crust to decreasing extents during ascent and differentiation. Due to a Cretaceous thermal event, $^{40}\text{Ar}/^{39}\text{Ar}$ -ages (ranging from 235 to 90 Ma) and S-isotope characteristics are heavily disturbed, only a few samples exhibit the relict primary $\delta^{34}\text{S}$ -value of -19.5 .

3 The Andean Subduction Model and Its Embedding

3.1 *Some Fundamental Remarks*

Our modeling of the Andean slab should be compatible with our basic assumption that plate tectonics is an integral part of the convection of the entire mantle. Therefore, we should aim at a regional model which is embedded into a realistic convective spherical-shell model. It is possible that the mantle convection is characterized by top-down control. But it is also possible that the larger part of the mantle mass essentially determines the movements at the surface since the most important share of the primordial energy is stored there and also the principal share of the radiogenic energy is released there. Here we refer to the absolute value, not to the density of these quantities. On the other hand, for reasons of energy, it is evident that the Earth's core cannot play a prominent part in controlling mantle convection. It is exactly the reverse. The mantle convection determines the boundary conditions of the hydromagnetic convection in the outer core. For example, in time spans of high activity of mantle convection, the latter one generates lateral temperature differences in D'' which reduce the number of magnetic reversals or even make them impossible because of the anti-dynamo theorems.

Furthermore, it is well known at the present time that the oceanic lithosphere consists of three (or more) layers which are chemically different and that its lower boundary is characterized by a sharp viscosity jump. At the same time the oceanic lithosphere is also a thermal boundary layer. So, we do not intend to use the old simplified approach that the existence of an oceanic lithosphere can *exclusively* be explained by a thermal boundary layer. In this case we should expect a gradual decrease of the viscosity at the lower boundary. Furthermore, we conclude that the principal part of the buoyancy of the slab heavily depends on chemistry and that phase transitions, especially the basalt-eclogite transition, play an eminent role.

So, we want to combine a global 3-D spherical-shell convection model with a 3-D regional convection model of South America and the surrounding plates and a model of the orogeny of the Cordilleras. The Andes are an ideal test case for various reasons:

- They are very large, thus keeping the inevitable problems of different scales at a minimum.
- They are active and well-studied. A wealth of information constrains the processes of orogenesis.
- They have a simple large-scale geometry. The plate margin is gently curved and was even straighter in the past. Convergence is orthogonal to the mean trend of the margin. The age structure of the Nazca plate near the contact with South America is symmetric, with the oceanic lithosphere oldest in the center and younging to both sides.
- Their plate kinematic framework has remained nearly unchanged for the last 50 Ma. On the other hand, there was a prominent switch in the mode of subduction earlier, from presumably steep with backarc extension to low-angle with backarc shortening. In the Andes, both end-member settings can therefore be studied in the same place.
- There is a clear compositional and rheological contrast between the two converging plates. It is unlikely that large volumes of material are transferred across the plate contact, in strong contrast to continental collision zones.
- The Andean substrate has a simple geologic history. Much of the South American plate was in place before subduction started some 200 Ma ago. Except for the northern Andes, no terranes were accreted after the Paleozoic.

We aim at a numerical, nearly purely dynamic model with a minimum number of restrictions and additional assumptions. This model is to explain the physical mechanism of the essential features of Andean orogeny.

3.2 A Model of the Andean Subduction

Outlines of the Model

We do not develop an exclusively regional model of the Andean orogenesis since, in this case, the temporally varying boundary conditions are unknown. Therefore, it is often assumed, for reasons of simplicity, that there are no effects from outside of the regional computational domain. However, some changes in the arc volcanism and in the tectonic shortening of the Andes suggest a connection with the 30-Ma Africa-Eurasia collision. Therefore, we embed a regional 3D model into a 3D spherical-shell model. So, we solve the balance equations of momentum, energy and mass in the spherical-shell model using somewhat larger time steps on a coarser whole-mantle grid, coarser than in the regional model. The values of creeping velocity, temperature and pressure, determined in that way and lying at the boundaries of the *regional* computational domain, then serve as boundary conditions for a computation with smaller time steps for which the balance equations are solved in the regional computational domain.

3.2.1 The Regional Model

Meanwhile, we have developed a numerical tool for several classes of regional models, and it was indeed a great effort. *So, we are in no way restricted to the model developed in the following.* We could as well compare the effects of different geological proposals. To design the regional model, we developed not only extensive numerical improvements (see Sect. 2.2) in the Terra code but studied also the latest geophysical, geological and geochemical results taking them into consideration in the draft of a physically reliable mechanism which is not only geodynamically probable but also numerically feasible (U. Walzer, J. Kley, L. Viereck-Götte). There are several geologically descriptive model proposals. We mention only [13, 28, 29, 37, 71, 76]. Our designed computable model system ought to solve the following problems.

- Why do we observe today in some segments of the Andes flat subduction and magmatic lull {Bucaramanga, Peruvian (2–15°S) and Pampean (27–33°S) flat slab [75]}, but in other segments normal subduction with dip angles between 30° and 40°? This is amazing since the westward velocity of the South American plate and the eastward velocity of the Nazca plate do not *essentially* vary alongshore.
- Why do the flat-slab segments migrate in Cenozoic times along-side the Andes [76]? Ramos and Folguera [77] found an almost continuous belt of flat slabs which migrate southward.
- Why is the present-time volcanism restricted to segments with a 30–40° dipping slab [1, 36, 48, 83]?
- Why does the deformation essentially start in the West and migrate to and finish in the East [71]? We derived some estimations on some other hypotheses. After that we consider the assumption as most promising to answer the mentioned questions by the assumption that oceanic plateaus and aseismic ridges are carried by the conveyor belt, i.e. by the Nazca plate. The plateaus and ridges generate additional positive buoyancy [27]. So the hinge of the slab migrates to the East until the volcanism totally vanishes. However, if we scrutinize a good geological map of South America we notice that the relation between flat-slab segments and ridges are not simple. We can assign the Pampean flat slab to the Juan Fernandez Rigde [2]. Even the southward migration of the Pampean flat-slab zone can be explained by form and movement of the Juan Fernandez Rigde [37]. The southern part of the Peruvian flat slab can be referred to the Nazca Rigde. For the northern part of the Peruvian flat slab we have to introduce the hypothesis of an immersed Inca Plateau [28]. However, east of the Carnegie Rigde there is an abundant volcanism in Ecuador. Michaud et al. [64] show a detailed reconstruction of the eastward movement of the Carnegie Rigde which extends at least 60 km below the South American plate with a continuous plunging slab down to a depth of 200 km. The adakitic signal is proposed to be ridge-induced. In the case of the Iquique rigde we have to assume that there is no eastern continuation of it. Pindell

and Kennan [74] show that the flat-slab area in northern Colombia and Venezuela might be considerably larger than the area assumed by Ramos [76].

- *Why should our mechanism of the generation of the Andes be three-dimensional?* Several observations suggest the idea that essential features of the Andean orogenesis cannot be explained by 2-D dynamical models:
 - (a) Hindle et al. [33] conclude that a mass balance which is restricted to a cross-section through the Andes leads into contradictions. They show that there has to exist an essential mass transport alongside the Andes. In particular, the displacement of material toward the axis of the bend in the central Andes leads to a significant crustal thickening. This cannot be explained by a two-dimensional model, neither kinematically nor dynamically.
 - (b) Anderson et al. [3], Kneller and van Keken [53] and Barnes and Ehlers [5] show and discuss, for the southern Andean subduction zones, trench-parallel high seismic shear velocities near to the trench and an abrupt transition to trench-perpendicular high seismic shear velocities in the back arc. The Brazilian subcrustal lithosphere beneath the eastern Cordillera, the Interandean and the Subandes are East-West fast whereas the shear-wave velocity under the Altiplano and Puna has maximum values in the North-South direction. This is a hint that a significant three-dimensional flow might be involved in the mechanism.
 - (c) *The toroidal component.* A pertinent argument for the necessity of 3-D models results from the following considerations and calculations. Already Gable et al. [20] and O'Connell et al. [70] showed the relevance of the toroidal-poloidal partitioning for lithospheric plate motions. The lateral subducting slab movement induces slab-parallel flows and a rollback-generated flow around the slab [81]. Stegman et al. [86] demonstrated that in the case of non-vanishing rollback of the subduction slab for some typical cases, 69 % of the energy of the negative buoyancy of the slab is converted into the toroidal component of the rollback-induced flow whereas 18 % are consumed for the weakening of the plate. These numbers show the importance of a 3-D modeling in a striking way. Only in the very beginning of the Andean-specific modeling we prescribe the velocity of the migrating subduction hinges as a function of time according to [71] in order not to overburden the model. But the other degrees of freedom of the flexible slab should be determined by the differential equations of the model. We vary the lateral extend of the individual slab between 200 and 5,000 km. That is, in a first type of numerical experiments we introduce the individual lobes shown by the distribution of seismicity. In a second numerical experiment we assume an undivided slab for the whole South American continent (Fig. 7), at best with a disconnection at the Chile Rise. For all versions we cut out a spherical diamond (Fig. 8) from the newly improved and inf-sup stable Terra code which is able to solve the convection differential equations in a spherical-shell mantle. Essential parts of the South American plate and the Nazca plate fit into this spherical diamond. The vertical boundary conditions are

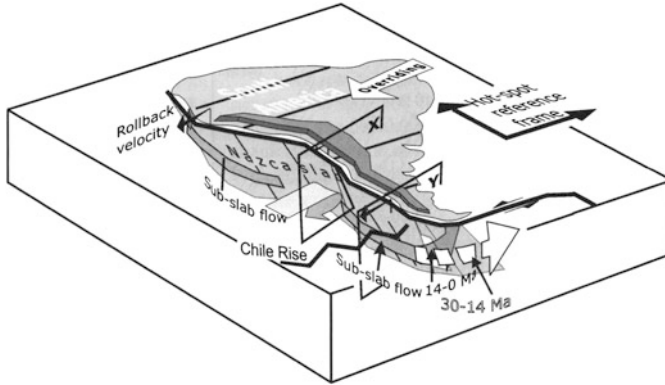


Fig. 7 The geometric starting configuration in our second Andean regional model (Taken from [92])

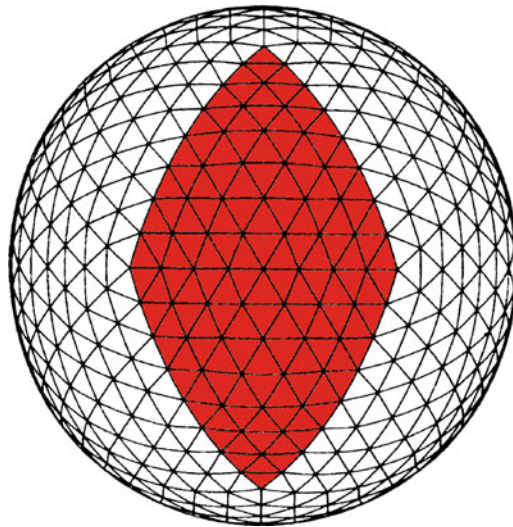


Fig. 8 The diamond (red), embedded in the global grid, which will be dyadically refined to the model resolution (Modified from [6, Fig. 1]). Of course, we use a further refinement of the grid

iteratively taken from a whole-mantle convection model. Cf. Sect. 3.2.2. In contrast with [86], we do not neglect the energy equation. It is evident that the subduction mechanism is possible only assuming a low-viscosity asthenosphere [18] which is less dense than the average oceanic lithosphere. Furthermore, the rheology may not be purely viscous. For this purpose, we [97] prefer a viscoplastic yield stress. The lithospheric-asthenospheric boundary for the viscosity is relatively sharp, also for the oceanic lithosphere. This is a special challenge for our code.

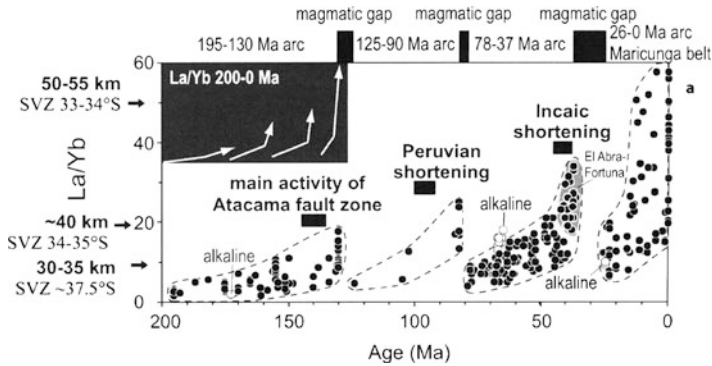


Fig. 9 The La/Yb ratio as a function of time for the igneous rocks of the north Chilean arc (21–26°S) acc. to Haschke et al. [29]. Note that *after* the flat-slab stage, the La/Yb *suddenly* decreases to a low starting value. The periods of orogenetic activity are *before* these drops

- *By the model, it should be possible to understand essential geochemical observations relevant for South America.* The difficult problem of delamination is very probably connected with this issue. It is necessary to clarify what kind of delamination is dominant. Figure 9 shows the gradual increase of the flow of incompatible elements. After each flat-slab period, this rise is abruptly interrupted. Such kind of plots exist not only for the mass ratio La/Yb but also for $^{87}\text{Sr}/^{86}\text{Sr}$ and $^{144}\text{Nd}/^{143}\text{Nd}$. These curves describe a slow growth of the abundances of elements with large ionic radii within one cycle since ^{87}Sr is the daughter isotope of ^{87}Rb , ^{143}Nd is the daughter isotope of ^{147}Sm and the other mentioned isotopes are stable. The fluctuations of the whole-rock initial ϵ_{Nd} of the central Andean arc by DeCelles et al. [13] are evidently related to Fig. 9. DeCelles et al. [13] emphasize that the cyclical changes of the isotopic compositions of arc magmas cannot be explained by changes in the convergence rates. They and also we expect that these changes have to be explained by episodic gravitational foundering. There are two principal possibilities.

(A) According to [13], below arc and hinterland, i.e. below the western parts of the South American continent, the eclogitization of the thickening lower continental crust and of the lithospheric mantle causes a density increase and therefore a delamination so that these units sink into the mantle wedge driven by their own weight. Carlson et al. [10] discuss the possibility that the continental mantle above the wedge of the mantle overlying a subducting oceanic plate can become unstable. The detachment from the overlying continental crust can cause major orogenetic episodes. Davidson and Arculus [11] propose a delamination of the cumulate layers below the seismological Moho back into the mantle of the sub-arc wedge. The two-dimensional numerical model by Sobolev et al. [84, 85] is compatible with the geological models mentioned under a) and belongs to b)-type of papers mentioned in the Introduction. They use a viscoelastic rheology supplemented by Mohr-

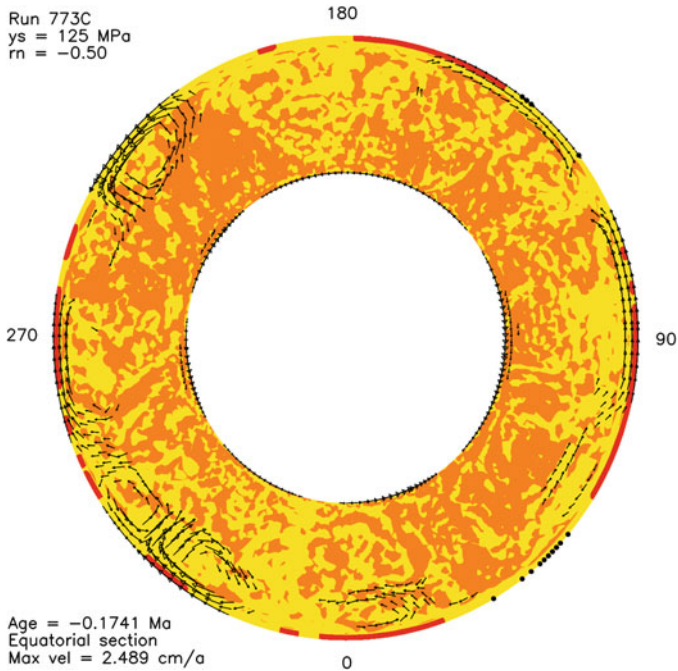


Fig. 10 A calculated marble-cake mantle model acc. to Walzer and Hendel [99]. This is an equatorial section showing the present-time state of the chemical evolution of incompatible elements of the Earth's mantle. We use a modernized reservoir theory. The depleted MORB mantle (DMM) and a mantle which is rich in incompatible elements, yet, are strongly intermixed. Strongly depleted parts of the mantle which include more than 50 % DMM are represented by *yellow areas*. Relatively rich mantle parts with less than 50 % DMM are *orange-colored*. In general, the *yellow-orange* boundary does *not* correspond to a discontinuity of the abundances of U,Th,K, etc. The cross sections through the continents are *red*. *Black dots* represent the oceanic plateaus. The yield stress is 125 MPa, the viscosity-level parameter is -0.50

Coulomb plasticity for the layered lithosphere. The drift of the overriding plate and the pulling of the slab is prescribed by the velocities at the boundaries of the 2-D model area and it is not calculated by solution of the balance equations though. What drives Andean orogeny? Sobolev et al. [84, 85] answer this question by numerical experiments using their 2-D model and varying only one influence parameter each. They conclude that the major factor is the westward drift of the South American plate. Paragraph (A) outlines only *one* way of thinking which we intend to test.

- (B) Here we propose a second hypothesis to understand the mentioned geochemical observations of [29] and of [13, Fig. 5]. This hypothesis is patronized by the idea of a geochemical marble-cake mantle [97, 99] (see Fig. 10) but composed of irregularly formed parts of a depleted MORB mantle (DMM) with 80–180 ppm H_2O and 50 ppm C and another, richer reservoir with 550–1,900 ppm H_2O and 900–3,700 ppm C [23, 111, 112]. The mid-oceanic ridge basalt is denoted by MORB. It is possible that the reservoirs are

intermixed in smaller quantities so that there is no sharp boundary between the different parts of the mantle [34, 89]. DMM dominates in the smaller depths of the mantle. The deeper the slab dives into the mantle, the higher is the probability to touch regions with a high abundance of ^3He and incompatible elements. Pilz [73] investigated $^3\text{He}/^4\text{He}$ ratios in the Puna plateau and at the volcano Tuzgle. He found that these $^3\text{He}/^4\text{He}$ values are higher than in the western Cordillera and in the Salta Basin east of it. Pilz and also we conclude that a provenance by degassing of the slab is not feasible since the mantle's ^3He is primordial. The ^3He of the atmosphere cannot be subducted in appreciable quantities.

There are different, but related models of chemical layering inside the subducting oceanic lithosphere [21, 80]. There is a water-rich subduction channel above the slab. Because of the sediment dehydration and the oceanic crustal dehydration it is not entirely clear how deep this hydrous channel is extended. Not only the $^3\text{He}/^4\text{He}$ ratio of the Puna plateau [73] but also La/Yb, $^{87}\text{Sr}/^{86}\text{Sr}$ and $^{144}\text{Nd}/^{143}\text{Nd}$ increase from an age of $\tau = 4.5$ Ma until the present time [29]. There are different explanations for this phenomenon. One of them would be a rise in an antiparallel direction in hot fingers immediately or in some distance above the subducting slab. Such a suggestion has been offered by Tamura et al. [91] for the NE Japanese arc. Marsh [63] proposed a similar idea of a hydrothermal flow field, in this case immediately above the upper surface of the down-going slab. In this way he explains also the sharp line of volcanoes or the volcanic front which can be observed in the Andes. Pilz [73] concludes from seismic observations that such hot fingers are also in the wedge of the southern central Andes and that these fingers are near the surface of the slab. So we want to develop a numerical model with fluid pathways of hydrothermal fluids, described by a particle approach, not very far from the slab but with an antiparallel flow direction. This idea is corroborated also by Furukawa [19].

We are working about the numerical problem to cut out a spherical diamond, out of the dynamical 3-D spherical-shell model, and to determine the temporally changing boundary conditions at the vertical side walls of the 3-D diamond by the solution of the convection in a spherical shell, but now with prescribed plates at the surface of the sphere. The Nazca plate moves with a (in the first approach) prescribed angular velocity through the margin into the computational domain and dives under the South American continent because of a Rayleigh-Taylor instability which is induced *mainly* by the transition to eclogite. The oceanic plate has a given sandwich structure of zero-pressure densities, ρ_0 , [21] and viscosities, η_0 . The slab is supposed to be freely movable at the surface and floating inside the mantle. It is well-known that it is difficult to detach a spherical-shell plate from the surface of the shell into the mantle in a slab-like manner [8]. As in [97], we want to introduce a viscoplastic yield stress at the near-surface lithospheric region and compare the creeping viscosity, η_c , at each position and time with the plastic viscosity, η_p , and use the minimum value in the model. This procedure is sensible from the physical point of view. If a piece of the Nazca plate which is thickened by an oceanic plateau

or a passive ridge approaches to South America then it pushes the hinge back under the South American plate because of its positive buoyancy. Therefore the volcanic front migrates to the East. The residual slab will become steeper and its tip will touch deeper and deeper parts of the mantle. Therefore, more and more atoms of incompatible elements will rise using the fluid pathways explaining the rising parts of the curve of Fig. 9. We are able to describe the movements of the hydrothermal fluid by a tracer modulus. These particles, describing the migration velocities of higher abundances of incompatible elements, ^3He , metals like Cu, Ag, etc., are *not* carried along with the creeping rock. They can move along a surface antiparallel to the slab which represents a thin layer. A serpentinized layer-like part of the mantle wedge just above the subducting oceanic crust could serve in reality as such a thin layer [25]. The slab movement is (in this model as in reality) an integral part of the solid-state mantle convection. The mentioned quantities ρ_0 and η_0 of the slab will be additionally described by other tracers which, in this case, will be entrained and carried along by the solid-state creep down to the interior of the mantle. The generation and eastward migration of major Andean ore deposits [29,38,39,79], the eastward migration of the volcanic front, the eastward movement of the deformation ages across the southern central Andes (21°S) [17,71] as well as the eastward migration of deformation in the Interandean and Subandean [16,41] can be dynamically modeled by our approach. When the subducting movement of the down-hanging part of the slab (and the flat-slab part behind) is accelerated, then an elevated activity of the Atacama fault zone, the Peruvian shortening, the Incaic shortening etc. are induced. The sudden interruption of the supply of highly incompatible elements (Fig. 9) must be induced by a radical event. Using the analogous, geologically describing models of [59, Fig. 4] and [35, Fig. 7], it cannot be concluded that many unusual features of the Permian-Jurassic South China fold belt can be explained by shallow subduction with an extensive final foundering of the lower plate combined with a roll-back of a small remnant subducting slab in the Mid-Jurassic. Humphreys [35] concludes for the Mid-Tertiary that an extensive sinking of the flat Farallon slab occurred which caused an uplifting of the continent covering a large area of the western North America. We propose an explanation by an extensive generalized eclogitization of the flat-slab part of the oceanic plate and an *extensive* delamination due to a Rayleigh-Taylor instability. The latter process can be simulated for the former and present South American flat slabs using a particle approach. The extensive tear-off would entirely interrupt the supplies of incompatible elements, ^3He , etc. since the tracer transport path near the upper surface of the low-hanging part of the slab and the flat part of the slab is ripped.

At first glance, (A) and (B) seem to be competing models, but in reality they do not entirely exclude one another. It is evident that the two roughly sketched numerical regional models are very ambitious. Therefore, we could report here only on the numerical and mathematical results of the preparatory efforts, the further development of the code and our geodynamical conception. However, a spherical-shell model is finished (cf. 2.1).

3.2.2 Spherical-Shell Model: Prescribed Angular Velocities of the Lithospheric Plates

To define the time-dependent boundary conditions of the vertical side walls of the spherical diamond containing South America and the Nazca plate, we introduce a spherical-shell convection model with the same radial profiles of the relevant physical parameters as in [100, 101] but with prescribed angular velocities of the plates for the last 200 Ma. This desirable time span is essentially determined by the available observational data, e.g. by Fig. 9. But the most plate-motion models do not go back so far. However, the main difficulty refers to another item. Even though we know all velocities of neighboring plates between each other, we do not know the “absolute” velocities of the plates relative to the highly viscous mid part of the lower mantle. But the net rotation of the averaged lithosphere is important for the kinematic analysis and the dynamic modeling of the slabs, especially the slabs at the margin of South America. The “global tectonic map” of [82] is based on the Indo-Atlantic hotspot reference frame by O’Neill et al. [72] and on the relative plate motion model by DeMets et al. [14]. This map shows a large eastward motion of the Nazca plate, large in comparison to the magnitude of the velocity of the South American plate. In relation to this feature, this map is similar to the deforming, no-net-rotation reference frame model GSRM by Kreemer et al. [56]. In contrast to these two models, the hotspot reference model HS-3 [24] shows a high westward velocity of the South American plate, high in comparison with the amount of the velocity vectors of the Nazca plate. HS-3 is based on the age progressions of ten Pacific ocean islands. Becker [7] and Becker and Faccenna [8] wrote a very good analysis of the problem of “absolute” plate velocities. Becker [7] and Long and Becker [62] try to determine the present-day plate velocities from the convective shearing movements and the seismic anisotropy of the upper mantle. But this procedure is more sensitive to the direction of the velocity vector than to its magnitude. HS-3 contains a large net rotation of the laterally averaged lithosphere relative to the high-viscosity parts of the lower mantle. The majority of the authors derived a smaller real net rotation which is defined as the spherical harmonic degree $l = 1$ component of the toroidal part of the plate velocities. Ricard et al. [78] estimated 30 % of HS-3, Steinberger et al. [88] calculated 38 %. The azimuthal seismic anisotropy is compatible only with values less than 50 % of HS-3 [7].

Already early, Steinberger and O’Connell [87] linked the hot spot tracks and the movement of oceanic lithospheric plates. Gurnis et al. [26] report on a very practicable open-source system which contains the angular velocities for the plates from 140 Ma to the present time. Each plate has a time-dependent Euler pole. The plates are described by time-dependent closed plate polygons. Each of these plate boundaries has its own, time-dependent Euler pole. The code allows to introduce new interactive plate boundaries [9]. We intend to use two or three seemingly realistic spherical-shell plate-motion models to define the boundary conditions of our regional convective system of South America and its surrounding. The repercussions of the different spherical-shell systems on the regional model should be investigated and compared.

3.2.3 Future Numerical and Technical Improvements

In addition to the joint work within the group of Terra developers, further developments are to be continued regarding the following items.

- We are going to further improve the parallelization of the particle tracking routines in Terra. Compared to previous Terra versions, there is an extra need for communication among several MPI-processes to figure out connected regions of partial melting in the mantle from which incompatible elements are extracted and transported to the surface. A similar communication is required to define the extent of continental lithospheric plates. With the high number of tracers, it is crucial to compress the required global information locally before it is exchanged among neighboring processors. R. Hendel will continue to reduce the communication overhead for tracking globally connected regions, so that the scalability of the particle routines will be extended to 500 and more processors. Such an optimized way of communicating global regions and features is also needed in modeling the elasticity of the subducting plates in the regional Andean model.
- We also plan to bring the elasticity model in Terra to work. It has also to be chosen carefully how elasticity is dealt with in the solution of mass and momentum equations. It could be necessary to iterate over the whole Stokes within every time step until an equilibrium between elastic and viscous forces is reached.
- To run both, regional and global models, with time-dependent boundary conditions at the surface, plate reconstruction data will be imported from the GPlates code [9] (www.gplates.org). The development of the interface between GPlates and Terra will be done together with L. Quevedo, Sydney.
- Furthermore, the documentation of the code, which is build from source code comments automatically with doxygen, will be enhanced to make it easier for new developers to work on Terra.

Acknowledgements We gratefully acknowledge the stimulating discussions with J. Baumgardner, H.-P. Bunge, P. Bollada, H. Davies, R. Davies and M. Mohr in the group of Terra developers. We thank the Steinbuch Center for Computing, Karlsruhe, for the supply of computational time under grant sphshell. This work was partly supported by the Deutsche Forschungsgemeinschaft under grant KL 495/16-1.

References

1. R. W. Allmendinger, T. E. Jordan, S. M. Kay, and B. L. Isacks. The evolution of the Altiplano-Puna plateau of the Central Andes. *Annu. Rev. Earth Planet. Sci.*, 25: 139–174, 1997.
2. P. Alvarado, M. Pardo, H. Gilbert, S. Miranda, M. Anderson, M. Saez, and S. Beck. Flat-slab subduction and crustal models for the seismically active Sierras Pampeanas region of Argentina. In S. M. Kay and V. A. Ramos, editors, *Backbone of the Americas: Shallow subduction, Plateau Uplift, and Ridge and Terrane Collision*, pages 261–278. Geol. Soc. Am., 2009.

3. M. L. Anderson, G. Zandt, E. Triep, M. Fouch, and S. Beck. Anisotropy and mantle flow in the Chile-Argentina subduction zone from shear wave splitting analysis. *Geophys. Res. Lett.*, 31: L23608, 2004. doi: 10.1029/2004GL020906.
4. C. Arriagada, P. Roperch, C. Mpodozis, and P. R. Cobbold. Paleogene building of the Bolivian orocline: Tectonic restoration of the central Andes in 2-D map view. *Tectonics*, 27: 1–29, 2008. doi: 10.1029/2008TC002269.
5. J. B. Barnes and T. A. Ehlers. End member models for Andean Plateau uplift. *Earth Science Reviews*, 97: 105–132, 2009.
6. J. R. Baumgardner and P. O. Frederickson. Icosahedral discretization of the two-sphere. *SIAM J. Numer. Anal.*, 22: 1107–1115, 1985.
7. T. W. Becker. Azimuthal seismic anisotropy constrains net rotation of the lithosphere. *Geophys. Res. Lett.*, 35: L05303, 2008. doi: 10.1029/2007GL032928.
8. T. W. Becker and C. Faccenna. A review of the role of subduction dynamics for regional and global plate motions. In S. Lallemand and F. Funiciello, editors, *Subduction Zone Geodynamics*, pages 3–34. Springer, 2009. doi: 10.1007/978-3-540-87974-9.
9. J. Boyden, R. D. Müller, M. Gurnis, T. Torsvik, J. Clark, M. Turner, H. Ivey-Law, R. Watson, and J. S. Cannon. Next-generation plate-tectonic reconstructions using GPlates. In G. R. Keller and C. Baru, editors, *Geoinformatics: Cyberinfrastructure for the Solid Earth Sciences*, pages 95–113. Cambridge Univ. Press, 2011.
10. R. W. Carlson, D. G. Pearson, and D. E. James. Physical, chemical, and chronological characteristics of continental mantle. *Rev. Geophys.*, 43: RG1001, 24 pp., 2005. doi: 10.1029/2004RG000156.
11. J. P. Davidson and R. J. Arculus. The significance of Phanerozoic arc magmatism in generating continental crust. In M. Brown and T. Rushmer, editors, *Evolution and Differentiation of the Continental Crust*, pages 135–172. Cambridge Univ. Press, Cambridge, UK, 2006.
12. J. H. Davies and D. R. Davies. Earth’s surface heat flux. *Solid Earth*, 1: 5–24, 2010.
13. P. G. DeCelles, M. N. Ducea, P. Kapp, and G. Zandt. Cyclicity in Cordilleran orogenic systems. *Nature Geosci.*, 2: 251–257, 2009. doi: 10.1038/NGEO469.
14. C. DeMets, R. Gordon, D. Argus, and S. Stein. Effect of recent revisions to the geomagnetic reversal time scale on estimates of current plate motions. *Geophys. Res. Lett.*, 21: 2191–2194, 1994.
15. C. Dohrmann and P. Bochev. A stabilized finite element method for the Stokes problem based on polynomial pressure projections. *Int. J. Num. Meth. Fluids*, 46: 183–201, 2004.
16. H. Ege. *Exhumations-und Hebungsgeschichte der zentralen Anden in Südbolivien (21° S) durch Spaltspur-Thermochronologie an Apatit*. PhD thesis, Freie Univ. Berlin, 2004.
17. K. Elger, O. Oncken, and J. Glodny. Plateau-style accumulation of deformation: Southern Altiplano. *Tectonics*, 24: TC4020, 2005. doi: 10.1029/2004TC001675.
18. K. M. Fischer, H. A. Ford, D. L. Abt, and C. A. Rychert. The lithosphere-asthenosphere boundary. *Annu. Rev. Earth Planet. Sci.*, 38: 551–575, 2010.
19. Y. Furukawa. Convergence of aqueous fluid at the corner of the mantle wedge: Implications for a generation mechanism of deep low-frequency earthquakes. *Tectonophysics*, 469: 85–92, 2009.
20. C. W. Gable, R. J. O’Connell, and B. J. Travis. Convection in three dimensions with surface plates: Generation of toroidal flow. *J. Geophys. Res.*, 96: 8391–8405, 1991.
21. J. Ganguly, A. M. Freed, and S. K. Saxena. Density profiles of oceanic slabs and surrounding mantle: Integrated thermodynamic and thermal modeling, and implications for the fate of slabs at the 660 km discontinuity. *Phys. Earth Planet. Int.*, 172: 257–267, 2009.
22. K.-D. Gottschaldt, U. Walzer, R. Hendel, D. R. Stegman, J. R. Baumgardner, and H.-B. Mühlhaus. Stirring in 3-D spherical models of convection in the Earth’s mantle. *Philosophical Magazine*, 86: 3175–3204, 2006.
23. D. H. Green and T. J. Falloon. Pyrolyte: a Ringwood concept and its current expression. In I. Jackson, editor, *The Earth’s Mantle. Composition, Structure and Evolution*, pages 311–378. Cambridge Univ. Press, Cambridge, UK, 1998.

24. A. E. Gripp and R. G. Gordon. Young tracks of hotspots and current plate velocities. *Geophys. J. Int.*, 150: 321–361, 2002.
25. S. Guillot, K. Hattori, P. Agard, S. Schwartz, and O. Vidal. Exhumation processes in oceanic and continental subduction contexts: a review. In S. Lallemand and F. Funicello, editors, *Subduction Zone Geodynamics*, pages 175–205. Springer, 2009. doi: 10.1007/978-3-540-87974-9.
26. M. Gurnis, M. Turner, L. DiCaprio, S. Spasojević, R. D. Müller, J. Boyden, M. Seton, V. C. Manea, and D. J. Bower. Plate tectonic reconstructions with continuously closing plates. *Computers & Geosciences*, 38: 35–42, 2012.
27. M. A. Gutscher. Andean subduction styles and their effect on thermal structure and interplate coupling. *J. South Amer. Earth Sci.*, 15: 3–10, 2002.
28. M. A. Gutscher, W. Spakman, H. Bijwaard, and E. Engdahl. Geodynamics of flat subduction: Seismicity and tomographic constraints from the Andean margin. *Tectonics*, 19: 814–833, 2000.
29. M. Haschke, A. Günther, D. Melnick, H. Echtler, K. Reutter, E. Scheuber, and O. Oncken. Central and southern Andean tectonic evolution inferred from arc magmatism. In O. Oncken et al., editors, *The Andes*, pages 337–353. Springer, Berlin, 2006.
30. A. Heuret and S. Lallemand. Plate motions, slab dynamics and back-arc deformation. *Phys. Earth Planet. Int.*, 149: 31–51, 2005.
31. D. Hindle and J. Kley. Displacements, strains and rotations in the Central Andean plate boundary zone. In S. Stein and J. T. Freymuller, editors, *Plate boundary zones*, Geodynamics Series 30, pages 135–144. AGU, Washington, D. C., 2002.
32. D. Hindle, J. Kley, E. Klosko, S. Stein, T. Dixon, and E. Norabuena. Consistency of geologic and geodetic displacements during Andean orogenesis. *Geophys. Res. Lett.*, 29: 1188, 2002. doi: 10.1029/2001GL013757.
33. D. Hindle, J. Kley, O. Oncken, and S. Sobolev. Crustal balance and crustal flux from shortening estimates in the Central Andes. *Earth Planet. Sci. Lett.*, 230: 113–124, 2005.
34. A. W. Hofmann. Sampling mantle heterogeneity through oceanic basalts: Isotopes and trace elements. In R. W. Carlson, editor, *Treatise on Geochemistry, Vol.2: The Mantle and the Core*, pages 61–101. Elsevier, Amsterdam, 2003.
35. E. Humphreys. Relation of flat subduction to magmatism and deformation in the western United States. In S. M. Kay and V. A. Ramos, editors, *Backbone of the Americas: Shallow subduction, Plateau Uplift, and Ridge and Terrane Collision*, pages 85–98. Geol. Soc. Am., 2009.
36. S. M. Kay and J. M. Abbruzzi. Magmatic evidence for Neogene lithospheric evolution of the central Andean “flat-slab” between 30S and 32S. *Tectonophysics*, 259 (1–3): 15–28, 1996.
37. S. M. Kay and B. L. Coira. Shallowing and steepening subduction zones, continental lithospheric loss, magmatism, and crustal flow under the Central Andean Altiplano-Puna Plateau. In S. M. Kay and V. A. Ramos, editors, *Backbone of the Americas: Shallow subduction, Plateau Uplift, and Ridge and Terrane Collision*, pages 229–259. Geol. Soc. Am., 2009.
38. S. M. Kay and C. Mpodozis. Central Andean ore deposits linked to evolving shallow subduction systems and thickening crust. *GSA Today*, 11 (3): 4–9, 2001.
39. S. M. Kay, C. Mpodozis, and B. Coira. Neogene magmatism, tectonism, and mineral deposits of the Central Andes (22 degrees to 33 degrees S latitude). In B. J. Skinner, editor, *Geology and Ore Deposits of the Central Andes. Soc. Econom. Geol. Spec. Pub. 7*, pages 27–59. 1998.
40. J. Kley. Der Übergang vom Subandin zur Ostkordillere in Süd Bolivien (21 15–22 S): Geologische Struktur und Kinematik. *Berliner geowiss. Abh. (A)*, 156: 1–88, 1993.
41. J. Kley. Transition from basement-involved to thin-skinned thrusting in the Cordillera Oriental of southern Bolivia. *Tectonics*, 15 (4): 763–775, 1996.
42. J. Kley. Structural styles of foreland deformation in the Andes. *Z. dt. geol. Ges.*, 149: 13–26, 1998.
43. J. Kley. Geologic and geometric constraints on a kinematic model of the Bolivian orocline. *J. South Amer. Earth Sci.*, 12: 221–235, 1999.

44. J. Kley and C. R. Monaldi. Tectonic shortening and crustal thickness in the Central Andes: How good is the correlation? *Geology*, 26: 723–726, 1998.
45. J. Kley and C. R. Monaldi. Estructura de las Sierras Subandinas y del Sistema de Santa Bárbara. In G. González Bonorino, R. Omarini, and J. Viramonte, editors, *Geología del Noroeste Argentino*, volume 1, pages 415–425. Salta, 1999.
46. J. Kley and C. R. Monaldi. Tectonic inversion in the Santa Barbara System of the central Andean foreland thrust belt, northwestern Argentina. *Tectonics*, 21: 1061, 2002. doi: 10.1029/2002TC902003.
47. J. Kley and M. Reinhardt. Geothermal and tectonic evolution of the Eastern Cordillera and the Subandean Ranges of southern Bolivia. In K.-J. Reutter, E. Scheuber, and P. J. Wigger, editors, *Tectonics of the southern Central Andes*, pages 155–170. Springer, Berlin, 1994.
48. J. Kley and T. Vietor. Subduction and mountain building in the central Andes. In T. Dixon and J. Moore, editors, *The Seismogenic Zone of Subduction Thrust Faults*, volume 2 of *MARGINS Theoretical and Experimental Earth Science Series*, pages 624–659. Columbia University Press, 2007.
49. J. Kley, J. Müller, S. Tawackoli, V. Jacobshagen, and E. Manutsoglu. Pre-Andean and Andean-age deformation in the eastern Cordillera of southern Bolivia. *J. South Amer. Earth Sci.*, 10 (1): 1–19, 1997.
50. J. Kley, C. R. Monaldi, and J. A. Salfity. Along-strike segmentation of the Andean foreland: Causes and consequences. *Tectonophysics*, 301: 75–94, 1999.
51. J. Kley, E. A. Rossello, C. R. Monaldi, and B. Habighorst. Seismic and field evidence for selective inversion of Cretaceous normal faults, Salta rift, Northwest Argentina. *Tectonophysics*, 399 (1–4): 155–172, 2005.
52. E. R. Klosko, S. Stein, D. Hindle, J. Kley, E. Norabuena, T. Dixon, and M. Liu. Comparison of GPS, seismological, and geological observations of Andean mountain building. In S. Stein and J. T. Freymuller, editors, *Plate boundary zones*, Geodynamics Series 30, pages 123–133. AGU, Washington, D. C., 2002.
53. E. A. Kneller and P. E. van Keken. Trench-parallel flow and seismic anisotropy in the Mariana and Andean subduction systems. *Nature*, 450: 1222–1225, 2007. doi: 10.1038/nature06429.
54. C. Köstler. *Iterative solvers for modeling mantle convection with strongly varying viscosity*. PhD thesis, Friedrich-Schiller-Univ. Jena, <http://www.igw.uni-jena.de/geodyn>, 2011.
55. C. Köstler, M. Müller, U. Walzer, and J. Baumgardner. Krylov solvers and preconditioners for variable-viscosity convection models. *Comp. Geosci.*, submitted, 2012.
56. C. Kreemer, W. Holt, and A. Haines. An integrated global model of present-day plate motions and plate boundary deformation. *Geophys. J. Int.*, 154: 8–34, 2003.
57. N. Kukowski and O. Oncken. Subduction erosion - the “normal” mode of fore-arc material transfer along the Chilean margin? In O. Oncken et al., editors, *The Andes*, pages 217–236. Springer, Berlin, 2006.
58. S. Lamb and P. Davis. Cenozoic climate change as a possible cause for the rise of the Andes. *Nature*, 425: 792–797, 2003.
59. Z. X. Li and X. H. Li. Formation of the 1300-km-wide intracontinental orogen and postorogenic magmatic province in Mesozoic South China: A flat-slab subduction model. *Geology*, 35 (2): 179–182, 2007. doi: 10.1130/G23193A.1.
60. K. Litasov and E. Ohtani. Phase relations and melt compositions in CMAS-pyrolite–H₂O system up to 25 GPa. *Phys. Earth Planet. Int.*, 134: 105–127, 2002.
61. K. D. Litasov. Physicochemical conditions for melting in the Earth’s mantle containing a C-O-H fluid (from experimental data). *Russian Geology and Geophysics*, 52: 475–492, 2011.
62. M. D. Long and T. W. Becker. Mantle dynamics and seismic anisotropy. *Earth Planet. Sci. Lett.*, 297: 341–354, 2010.
63. B. D. Marsh. Magmatism, magma, and magma chambers. In G. Schubert, editor, *Treatise on Geophysics*, volume 6, pages 276–333. Elsevier, 2007.
64. F. Michaud, C. Witt, and J. Y. Royer. Influence of the subduction of the Carnegie volcanic ridge on Ecuadorian geology: Reality and fiction. In S. M. Kay and V. A. Ramos, editors, *Backbone of the Americas: Shallow subduction, Plateau Uplift, and Ridge and Terrane Collision*, pages 217–228. Geol. Soc. Am., 2009.

65. J. X. Mitrovica and A. M. Forte. A new inference of mantle viscosity based upon joint inversion of convection and glacial isostatic adjustment data. *Earth Planet. Sci. Lett.*, 225 (1): 177–189, 2004.
66. P. Molnar and T. Atwater. Interarc spreading and Cordilleran tectonics as alternates related to the age of subducted oceanic lithosphere. *Earth Planet. Sci. Lett.*, 41: 330–340, 1978.
67. C. R. Monaldi, J. A. Salfity, and J. Kley. Preserved extensional structures in an inverted Cretaceous rift basin, northwestern Argentina: Outcrop examples and implications for fault reactivation. *Tectonics*, 27: C1011, 2008. doi: 10.1029/2006TC001993.
68. M. Müller. *Towards a robust Terra code*. PhD thesis, Friedrich-Schiller-Univ. Jena, <http://www.igw.uni-jena.de/geodyn>, 2008.
69. M. Müller and C. Köstler. Stabilization of the 3-D spherical convection code Terra. *Int. Jour. Num. Meth. Engng.*, submitted, 2012.
70. R. J. O'Connell, C. W. Gable, and B. H. Hager. Toroidal-polooidal partitioning of lithospheric plate motions. In R. Sabadini and other, editors, *Glacial Isostasy, Sea-Level and Mantle Rheology*, pages 535–551. Kluwer, Norwell, MA, 1991.
71. O. Oncken, D. Hindle, J. Kley, K. Elger, P. Victor, and K. Schemmann. Deformation of the central Andean upper plate system - facts, fiction, and constraints for plateau models. In O. Oncken et al., editors, *The Andes*, pages 3–27. Springer, Berlin, 2006.
72. C. O'Neill, D. Müller, and B. Steinberger. On the uncertainties in hot spot reconstructions and the significance of moving hot spot reference frames. *Geochem. Geophys. Geosys.*, 6: Q04003, 2005. doi: 10.1029/2004GC000784.
73. P. Pilz. *Ein neues magmatisch-tektonisches Modell zur Asthenosphärendynamik im Bereich der zentralandinen Subduktionszone Südamerikas*. PhD thesis, Universität Potsdam, 2008.
74. J. Pindell and L. Kennan. Tectonic evolution of the Gulf of Mexico, Caribbean and northern South America in the mantle reference frame: An update. *Geol. Soc. London*, 328: 1–55, 2009.
75. V. Ramos, E. Cristallini, and D. Pérez. The Pampean flat-slab of the Central Andes. *J. South Amer. Earth Sci.*, 15: 59–78, 2002.
76. V. A. Ramos. Anatomy and global context of the Andes: Main geologic features and the Andean orogenic cycle. In S. M. Kay and V. A. Ramos, editors, *Backbone of the Americas: Shallow subduction, Plateau Uplift, and Ridge and Terrane Collision*, pages 31–65. Geol. Soc. Am., 2009.
77. V. A. Ramos and A. Folguera. Andean flat-slab subduction through time. In B. Murphy et al., editors, *Ancient Orogens and Modern Analogues*, pages 31–54. Geol. Soc. London, 2009.
78. Y. Ricard, C. Doglioni, and R. Sabadini. Differential rotation between lithosphere and mantle: A consequence of lateral mantle viscosity variations. *J. Geophys. Res.*, 96: 8407–8415, 1991.
79. G. Rosenbaum, D. Giles, M. Saxon, P. G. Betts, R. F. Weinberg, and C. Duboz. Subduction of the Nazca Ridge and the Inca Plateau: Insights into the formation of ore deposits in Peru. *Earth Planet. Sci. Lett.*, 239: 18–32, 2005.
80. L. H. Rüpke, J. Phipps Morgan, M. Hort, and J. A. D. Connolly. Serpentine and the subduction zone water cycle. *Earth Planet. Sci. Lett.*, 223: 17–34, 2004.
81. W. P. Schellart. Kinematics of subduction and subduction-induced flow in the upper mantle. *J. Geophys. Res.*, 109: B07401, 2004. doi: 10.1029/2004JB002970.
82. W. P. Schellart and N. Rawlinson. Convergent plate margin dynamics: New perspectives from structural geology, geophysics and geodynamic modelling. *Tectonophysics*, 483: 4–19, 2010.
83. M. Sébrier and P. Soler. Tectonics and magmatism in the Peruvian Andes from late Oligocene time to the present. In R. S. Harmon and C. W. Rapela, editors, *Andean Magmatism and its Tectonic Setting*, volume 265 of *Geol. Soc. Am. Spec. Paper*, pages 259–278. Geol. Soc. of America, Boulder, Col., 1991.
84. S. Sobolev, A. Babeyko, I. Koulakov, and O. Oncken. Numerical study of weakening processes in the central Andean back-arc. In O. Oncken et al., editors, *The Andes*, pages 513–535. Springer, Berlin, 2006.
85. S. V. Sobolev and A. Y. Babeyko. What drives orogeny in the Andes? *Geology*, 33 (8): 617–620, 2005.

86. D. Stegman, J. Freeman, W. Schellart, L. Moresi, and D. May. Influence of trench width on subduction hinge retreat rates in 3-D models of slab rollback. *Geochem. Geophys. Geosys.*, 7: Q03012, 2006. doi: 10.1029/2005GC001056.
87. B. Steinberger and R. J. O'Connell. Advection of plumes in mantle flow: Implications for hotspot motion, mantle viscosity and plume distribution. *Geophys. J. Int.*, 132: 412–434, 1998.
88. B. Steinberger, R. Sutherland, and R. J. O'Connell. Prediction of Emperor-Hawaii seamount locations from a revised model of global plate motion and mantle flow. *Nature*, 430: 167–173, 2004.
89. A. Stracke, A. W. Hofmann, and S. R. Hart. FOZO, HIMU and the rest of the mantle zoo. *Geochem. Geophys. Geosys.*, 6: Q05007, 2005. doi: 10.1029/2004GC000824.
90. P. J. Tackley. Modelling compressible mantle convection with large viscosity contrasts in a three-dimensional spherical shell using the yin-yang grid. *Phys. Earth Planet. Int.*, 171: 7–18, 2008.
91. Y. Tamura, Y. Tatsumi, D. Zhao, Y. Kido, and H. Shukuno. Hot fingers in the mantle wedge: New insights into magma genesis in subduction zones. *Earth Planet. Sci. Lett.*, 197: 105 – 116, 2002.
92. T. Vietor and H. Echtler. Episodic Neogene southward growth of the Andean subduction orogen between 30° S and 40° S - Plate motions, mantle flow, climate, and upper-plate structure. In O. Oncken et al., editors, *The Andes*, pages 375–400. Springer, Berlin, 2006.
93. U. Walzer and R. Hendel. Time-dependent thermal convection, mantle differentiation, and continental crust growth. *Geophys. J. Int.*, 130: 303–325, 1997a.
94. U. Walzer and R. Hendel. Tectonic episodicity and convective feedback mechanisms. *Phys. Earth Planet. Int.*, 100: 167–188, 1997b.
95. U. Walzer and R. Hendel. A new convection-fractionation model for the evolution of the principal geochemical reservoirs of the Earth's mantle. *Phys. Earth Planet. Int.*, 112: 211–256, 1999.
96. U. Walzer and R. Hendel. A new convection-fractionation model for the evolution of the principal geochemical reservoirs of the Earth's mantle. *EOS Transactions*, 80 (46): F1171, 2000.
97. U. Walzer and R. Hendel. Mantle convection and evolution with growing continents. *J. Geophys. Res.*, 113: B09405, 2008. doi: 10.1029/2007JB005459.
98. U. Walzer and R. Hendel. Predictability of Rayleigh-number and continental-growth evolution of a dynamic model of the Earth's mantle. In S. Wagner, M. Steinmetz, A. Bode, and M. Brehm, editors, *High Perf. Comp. Sci. Engng. '07*, pages 585–600. Springer, Berlin, 2009.
99. U. Walzer and R. Hendel. A geodynamic model of the evolution of the Earth's chemical mantle reservoirs. In W. E. Nagel, D. B. Kröner, and M. M. Resch, editors, *High Perf. Comp. Sci. Engng. '10*, pages 573–592. Springer, Berlin, 2011.
100. U. Walzer and R. Hendel. Silicate Earth differentiation, 3-D spherical-shell mantle convection, and evolution of continents. *Earth Planet. Sci. Lett.*, submitted, 2012a.
101. U. Walzer and R. Hendel. Real episodic growth of continental crust or artefact of preservation? A 3-D geodynamic model. *J. Geophys. Res.*, submitted, 2012b.
102. U. Walzer, R. Hendel, and J. Baumgardner. Variation of non-dimensional numbers and a thermal evolution model of the Earth's mantle. In E. Krause and W. Jäger, editors, *High Perf. Comp. Sci. Engng. '02*, pages 89–103. Berlin, 2003.
103. U. Walzer, R. Hendel, and J. Baumgardner. Viscosity stratification and a 3D compressible spherical shell model of mantle evolution. In E. Krause, W. Jäger, and M. Resch, editors, *High Perf. Comp. Sci. Engng. '03*, pages 27–67. Springer, Berlin, 2004a.
104. U. Walzer, R. Hendel, and J. Baumgardner. The effects of a variation of the radial viscosity profile on mantle evolution. *Tectonophysics*, 384: 55–90, 2004b.
105. U. Walzer, R. Hendel, and J. Baumgardner. Generation of plate-tectonic behavior and a new viscosity profile of the Earth's mantle. In D. Wolf, G. Münster, and M. Kremer, editors, *NIC Symposium*, volume 20 of *NIC Series*, pages 419–428, Jülich, 2004c. Springer.

106. U. Walzer, R. Hendel, and J. Baumgardner. Toward a thermochemical model of the evolution of the Earth's mantle. In E. Krause, W. Jäger, and M. Resch, editors, *High Perf. Comp. Sci. Engng. '04*, pages 395–454. Springer, Berlin, 2005.
107. U. Walzer, R. Hendel, and J. Baumgardner. Plateness of the oceanic lithosphere and the thermal evolution of the Earth's mantle. In W. E. Nagel, W. Jäger, and M. Resch, editors, *High Perf. Comp. Sci. Engng. '05*, pages 289–304. Springer, Berlin, 2006.
108. U. Walzer, R. Hendel, and J. Baumgardner. Continental growth and thermal convection in the Earth's mantle. In W. E. Nagel, W. Jäger, and M. Resch, editors, *High Perf. Comp. Sci. Engng. '06*, pages 473–497. Springer, Berlin, 2007.
109. U. Walzer, R. Hendel, and J. Baumgardner. Whole-mantle convection, continent generation, and preservation of geochemical heterogeneity. In W. E. Nagel, D. B. Kröner, and M. M. Resch, editors, *High Perf. Comp. Sci. Engng. '07*, pages 603–645. Springer, Berlin, 2008.
110. U. Walzer, R. Hendel, C. Köstler, and J. Kley. Andean Orogeny and Plate Generation. In W. E. Nagel, D. B. Kröner, and M. M. Resch, editors, *High Perf. Comp. Sci. Engng. '08*, pages 559–583. Springer, Berlin, 2009.
111. B. J. Wood. The effect of H₂O on the 410-kilometer seismic discontinuity. *Science*, 268: 74–76, 1995.
112. B. J. Wood and A. Corgne. Mineralogy of the Earth: Trace elements and hydrogen in the Earth's transition zone and lower mantle. In G. Schubert, editor, *Treatise on Geophysics*, volume 2, pages 63–89. Elsevier, 2007.
113. D. Yamazaki and S.-I. Karato. Some mineral physics constraints on the rheology and geothermal structure of the Earth's lower mantle. *Am. Min.*, 86: 385–391, 2001.
114. W.-S. Yang and J. R. Baumgardner. A matrix-dependent transfer multigrid method for strongly variable viscosity infinite Prandtl number thermal convection. *Geophys. Astrophys. Fluid Dyn.*, 92: 151–195, 2000.
115. A. Yoneda, M. Osako, and E. Ito. Heat capacity measurement under high pressure: A finite element method assessment. *Phys. Earth Planet. Int.*, 174: 309–314, 2009.